Drug Delivery and Translational Research
https://doi.org/10.1007/s13346-019-00643-0

ORIGINAL ARTICLE

Macrophage polarization in wound healing: role of aloe vera/chitosan nanohydrogel

Fatemeh Ashouri[1] · Fatemeh Beyranvand[2] · Nasim Beigi Boroujeni[2] · Majid Tavafi[3] · Ali Sheikhian[4] · Ali Mohammad Varzi[4] · Somayeh Shahrokhi[4]

Abstract

The balance between M1 and M2 macrophages plays an important role in wound healing. Interestingly, this immune response can be modulated by natural biomaterials such as chitosan nanohydrogel (Ch) and aloe vera (AV). Therefore, we aimed to improve wound recovery response by exploiting the potential healing properties of Ch and AV. Wounds were created in rats and were treated daily with either saline (control), AV, Ch, or different ratios of AV (volume):Ch (weight) (1:1), (2:1), and (3:1). M1 (iNOS, TNF-α) and M2 (CD163, TGF-β) responses were analyzed at days 3, 7, 14, 21, and 28. Wound healing increased within the third and seventh days in AV-Ch (3:1) ($P < 0.001$ and $P < 0.002$, respectively). In the treated groups, immunohistochemistry of iNOS expression decreased on the third day ($P < 0.0001$) while CD163 increased ($P < 0.0001$) on the 3rd, 7th, and 14th days. The gene expression of TGF-β decreased on the third day in AV group ($P < 0.03$) and on the 21st and 28th days in Ch-treated group ($P < 0.00$). TNF-α expression decreased in AV, Ch, and AV-Ch (3:1 *v/w*) on the 14th and 28th days ($P < 0.00$). TGF-β and TNF-α proteins decreased on the 28th day compared to the control and AV-Ch (3:1 *v/w*), respectively. AV-Ch (1 and 3:1 *v/w*) and Ch resulted in optimum wound repair by decreasing M1 after 3 days and increasing M2 after 14. Thus, Ch nanohydrogel, especially in combination with 1:1 and 1:3 ratio to AV, could be a proper candidate for modulating macrophages in response to wound healing.

Keywords Aloe vera · Chitosan · Macrophage · Nanohydrogel · Wound

Introduction

Macrophages play a critical role in wound healing and repair. Macrophage polarization, i.e., the plasticity of macrophage, in terms of phenotype and function, is important in pathological condition such as wound. Classically activated macrophages also known as (M1) are proinflammatory and initiate immune cell recruitment following tissue injury. Alternatively activated macrophages (M2) help resolve the inflammation phase and repair damaged tissue [1, 2]. Therefore, the balance between M1 and M2 plays a critical role in the healing and remodeling of injured tissues.

The macrophage polarization is affected by various properties such as mechanical properties, topography, and surface chemistry [3]. Interestingly, biomaterials such as biodegradable polymers and biologic materials seem to influence the flexible nature of these macrophages in wound healing [4]. The physical and chemical nature of the biomaterial such as specific topographies and pore structures affects on final outcome [5]. For instance, chitosan (Ch) films produced higher IL-10 and TGF-β1 anti-inflammatory cytokines as indication of M2 [6]; however, three-dimensional scaffolds of Ch enhanced production of TNF-a and IL-12/IL-23 inflammatory M1 cytokines [7]. The lack of sufficient comparative studies on biomaterial effects on macrophage polarization does not provide a definite conclusion. Hence, we aimed to study macrophage polarization in biopolymer-treated wounds.

Electronic supplementary material The online version of this article (https://doi.org/10.1007/s13346-019-00643-0) contains supplementary material, which is available to authorized users.

✉ Somayeh Shahrokhi
shahrokhi_so@yahoo.com

[1] Student Research Committe, Lorestan University of Medical Sciences, Khorramabad, Iran

[2] Razi Herbal Medicines Research Center, Lorestan University of Medical Sciences, Khorramabad, Iran

[3] Department of Anatomy, School of Medicine, Lorestan University of Medical Sciences, Khorramabad, Iran

[4] Department of Immunology, School of Medicine, Lorestan University of Medical Sciences, P.O. Box: 381351698, Khorramabad, Iran

Published online: 21 May 2019

Ch, a natural polysaccharide, shows wide range of biological activity such as anti-microbial, biocompatibility, biodegradability, hemostasis, tissue engineering scaffolds, drug delivery, and wound healing [8, 9].

The immune-modulatory properties of Ch induce innate immune cells to release a wide range of pro- and anti-inflammatory cytokines, chemokines, and growth factors depending on Ch characteristic [10]. Stimulation of M1 macrophage by Ch is one of the early evidence regarding its impact on innate immunity [11]. Combining the advantages of hydrogel and nanoscale to produce nanohydrogel produces amplified benefit to biomedicine [12]. Thus, we aimed to develop Ch nanohydrogel for modulation of innate immunity, particularly macrophage, in wound healing. This will address a new potential application of Ch and its immunomodulatory roles.

Another natural polymer, aloe vera (AV), has shown to have epithelizing effects on damaged skin tissue [13] which accelerates wound healing [14]. Additionally, it has anti-inflammatory, immunomodulatory, and antimicrobial activity [13, 15, 16], which are critical during wound healing. Notably, its antimicrobial characteristics are important to prevent wound infection. For instances, it is protective against common opportunistic fungi such as *Candida albicans* [17, 18]. On the other hand, AV shows anti-inflammatory action via LPS-activated primary macrophage by reducing IL-8, TNF-α, IL-6, and IL-1β cytokine production in a dose-dependent manner [19]. This results into M2 macrophage activation and subsequently inflammation resolution and healing initiation. According to the aforementioned immunomodulatory features, current research endeavors on AV are studying its conjugation with synthetic and natural polymers; this was implemented by producing two- and three-dimensional matrices including hydrogels, nanofibers, and films [15, 20, 21]. However, how conjugation affects biological responses in vivo still needs investigation, as there is minimal evidence of its effects.

Accordingly, we hypothesized that Ch-AV crosslinking, i.e., covalent bond of Ch nanohydrogel chain to AV polymer could be a potential candidate to promote healing processes, while protecting the injury from infection via modulation of macrophage polarization.

Material and methods

Preparation and characterization of AV-Ch nanohydrogel

Preparation of Ch-sebacic acid nanohydrogel solution

Two grams of Ch (Sigma-Aldrich) was added to 100 ml of acetic acid 1% (Merck Millipore). After obtaining a uniform solution, 20 min of sonication was performed to obtain a 5000-ppm solution. Sebacic acid (Sigma-Aldrich) was added to Ch at a ratio of 50:100 in order to link half amino groups of Ch chains with sebacic acid carboxyl groups. Amin-carboxyl linkage at this ratio results into nanohydrogel formation. To complete the reaction, the suspension was on stirrer for 24 h. Then, PH reached to 8.5–9 by adding NAOH to complete nanohydrogel formation. The solution was centrifuged at 9000 rpm for 5 min to remove impurities and the supernatant was aspirated. The precipitate was washed once with deionized water and three times with ethanol.

To solubilize the pellet, diluted acetic acid in deionized water was added while stirring. The final pH was tested and stabilized at 3.5 to 4. The obtained nanohydrogel was sterilized by passing through a 0.2-μm filter.

Encapsulation of AV gel in chitosan nanohydrogel

AV leaves were sectioned into pieces after disinfecting, and the gel, extracted from within the leaves, was blended and homogenized. To further study the different ratios of AV and Ch combination, the AV extract was added to Ch nanohydrogel (10,000 ppm) in ratios of 3:1, 2:1, and 1:1 volume/weight (*v*/*w*), respectively. Afterwards, sonication was performed and the hydrophilic extract of AV was trapped within the nanohydrogel, i.e., covalently binding to amine groups of Ch.

Characterization of nanohydrogel

To further characterize the physical structure of the AV-Ch nanohydrogel compounds, (a) AV-Ch (1:1 *v*/*w*), (b) AV-Ch (2:1 *v*/*w*), and (c) AV-Ch (3:1 *v*/*w*) were imaged and studied by scanning electron microscope [4]. Acceleration was set to 26 kV, magnification at 40,000 times, and 1-μm scale in KYKY apparatus (SBC12 model).

Additionally, to study chemical structures and to confirm the covalent bonding of sebacic acid to Ch, and incorporation of AV, Fourier transmission spectrometry (FTIR) was used. For this purpose, FTIR spectra of AV and/or Ch-sebacic acid were carried out. For IR spectrometry, both combinations of dried films were prepared. This spectrum was then recorded using a spectrometer (Jasco, Tokyo, japan) FTIR-430 at 20 °C and in the range of 500–4000 cm^{-1}.

Antibacterial and antifungal assay

The intrinsic antimicrobial features of AV and Ch are essential for wound healing [22]. Therefore, to test the antibacterial and antifungal activity of our proposed Ch nanohydrogel/AV, antimicrobial assays were performed using a broth microdilution method in a 96 plate based on CLSI method [23]. The minimum inhibitory

concentration (MIC)—the lowest concentration of an antimicrobial ingredient that prevents the microbial growth—and minimum bactericidal concentration (MBC) or minimal fungicidal concentration (MFC)—the lowest concentration of an antibacterial/antifungal drug that results the bacterial or fungal killing—respectively—(MBC, MFC) were studied in Ch nanohydrogel and AV compounds. A stock was prepared from Ch nanohydrogel and AV compounds with sterile Mueller Hinton Broth (Merck, Germany) for bacteria and Peptone Dextrose Broth (Merck, Germany) for yeast (2000 μg/ml). The microorganism strains were grown overnight on LB agar and individual colonies picked from the plates were suspended in LB broth to match the 0.5 McFarland standard ($\sim 1.5 \times 10^8$ CFU/mL). Then, serial dilution of the compounds and bacterial or fungal strain were cultured, in 50 μL volumes into a 96-well microtiter plate. Corresponding negative control (DMSO) (Sigma-Aldrich) and positive controls (gentamicin, gram-negative bacteria and vancomycin, gram-positive bacteria (Sigma-Aldrich) and fluconazole, fungi (Sigma-Aldrich)) were used (Table 1). The microtiter plates were incubated at 37 °C for 24–72 h while shaking. 2,3,5-Triphenyltetrazolium chloride (Sigma-Aldrich) was used for visualization of the growth of microorganisms. Colorless wells were reported as MIC inhibition of microbial growth. MBC test and MFC were done by sub-culturing 5 μl from each MIC, colorless, well. The plates were then incubated for 24 or 48 h. Least concentration of each compound showing no visible growth on subculture was taken as MBC/MFC.

Creating wounds in animals

All the animals in this study were handled in accordance with the guidelines approved by Ethics Committee of Lorestan University of Medical Sciences, Iran. The procedures were performed according to the protocol of the Care and Use of Laboratory Animals. Adult male Wistar rats (8–10 weeks) weighing approximately 250 g were used in this study. The rats were kept at room temperature of 25 ± 2 °C. The animals were individually anesthetized. Following shaving and disinfection of their skin, two full thickness skin wounds of 1-cm^2 area were prepared by a punch at the dorsum of the animals. After recovery, the rats were housed individually in properly disinfected cages. The rats (total $n = 90$) were randomly divided into six groups ($n = 15$/group) and were assigned to a distinct daily treatment: normal saline (control), three different ratios of AV-Ch (1:1 *v*/*w*) (group 1), (2:1 *v*/*w*) (group 2), or (3:1 *v*/*w*) (group 3), Ch nanohydrogel (group 4), and AV (group 5). During this period, the animals were handled gently to minimize the stress and to acclimatized them to the laboratory environment. Following daily treatment of the wounds, on the 3rd, 7th, 14th, 21st, and 28th days post wound creation, three mice from each group randomly were euthanized, and the size of their wound area was recorded. Wound tissue was collected and further analysis, i.e., histology (Hematoxylin & Eosin (H&E) (Sigma-Aldrich), immunohistochemistry, and real-time PCR examination was performed. Furthermore, blood samples of the mice were collected to measure TNF-α and TGF-β protein in serum (Supplementary Fig. 1).

Histopathological evaluation

Formalin-fixed paraffin-embedded (FFPE) blocks were prepared from each wound sample. Sections were prepared in 5 μm thickness, including the area between the wound midpoint and the surgical border (hairy skin surrounding). Sections of all specimens were stained by H&E method. The prepared slides were studied with an Olympus (CX31) light microscope (Olympus, Center Valley, PA).

Immunohistochemistry

Sections (5 μm) of the FFPE blocks were stained for iNOS and CD163 via immunohistochemical method. Briefly, sections were de-paraffinized in xylene and rehydrated in a graded ethanol series. Antigen retrieval was performed by steam heating slides in citrate buffer in a microwave oven. The slides were washed twice in phosphate buffered saline (PBS) containing 0.3% triton after cooling for 5 min. To prevent nonspecific antibody binding, the slides were incubated for 60 min in 10% goat serum at room temperature. The sections were incubated in either anti-CD163 (Bio-Rad) or anti-iNOS (Novus Biologica) overnight at 4 °C.

After washing in PBS, the slides were incubated in horseradish peroxidase-conjugated secondary antibody for 60 min at 37 °C. Then, the slides were incubated for 20 min with 3,3′-diaminobenzidine (DAB) solution (Sigma-Aldrich). Following washing, the sections were dehydrated in increasing alcohol concentrations and mounted. The average of CD163 and iNOS-positive cells in 100 random fields of each slide was counted using the Image plus2 software.

Measuring the serum concentration of TNF-α and TGF-β cytokines

After wound creation, sera samples of rats on the 3rd, 7th, 14th, 21st, and 28th days were collected and stored at − 70 °C until tested. TNF-α (cytokine of M1) and TGF-β (cytokine of M2) concentrations were measured by Rat TNF-α Quantikine ELISA Kit (R&D systems) and Rat TGF-β1 platinum kit (eBioscience).

Table 1 Antibacterial and antifungal properties of AV and Ch

(a) Antibacterial properties

	Pseudomonas aeruginosa ATCC 27853		*Escherichia coli* ATCC 1177		*Salmonella typhi* PTCC 1609		*Staphylococcus aureus* ATCC 12600		*Bacillus cereus* PTCC 1154		*Listeria monocytogenes* ATCC 13932	
	MIC	MBC	MIC	MBC	MIC	MBC	MIC	MBC	MIC	MBC	MIC	MBC
Av-Ch (1:1)	1000	2000	1000	2000	250	1000	250	1000	1000	2000	500	1000
Av-Ch (2:1)	2000	> 2000	1000	1000	500	1000	1000	2000	2000	> 2000	1000	2000
Av-Ch (3:1)	2000	> 2000	> 2000	2000	1000	2000	1000	2000	2000	> 2000	1000	2000
Ch	2000	> 2000	> 2000	2000	500	2000	1000	2000	2000	> 2000	500	1000
AV	2000	> 2000	1000	> 2000	500	1000	500	1000	500	2000	1000	2000
Positive control	0.5	1	0.5	1	16	16	8	128	128	128	4	4

(b) Antifungal property

	Candida albicans PTCC 5027		*Candida glabrata* PTCC 5297		*Kluyveromyces marxianus* PTCC 5188	
	MIC	MFC	MIC	MFC	MIC	MFC
Av-Ch (1:1)	500	1000	1000	2000	250	250
Av-Ch (2:1)	2000	> 2000	2000	2000	1000	1000
Av-Ch (3:1)	2000	> 2000	2000	2000	1000	1000
Ch	2000	> 2000	2000	2000	500	> 2000
AV	1000	1000	1000	2000	500	1000
Positive control	64	128	128	128	1	8

The antimicrobial activity of AV/Ch was assessed with microdilution method. MIC considered as colorless wells represents no growth of the tested microorganisms. MBC and MFC were performed with sub-culturing of 5 μL from MIC and evaluating the bacteria/fungi growth. Positive control for gram-negative bacteria was gentamicin, vancomycin for gram-positive bacteria, and fluconazole for fungi. DMSO was used for negative control. MIC, minimal inhibitory concentration; MBC, minimal bactericidal concentration; MFC, minimal fungicidal concentration

Total RNA extraction and CDNA synthesis

RNA extraction from FFPE blocks was performed [24] Accordingly, the FFPE tissues were cut by microtome and were de-paraffinized by two rinses in xylene (3 min at 50 °C). The samples were centrifuged for 1 min at maximum speed, and then the supernatant was discarded. After washing in 100% ethanol twice (7500*g* for 5 min), the pellets were dried at room temperature for 2–3 min. The 1× protease K digestion buffer containing 500 μg/ml protease K (Thermo Fisher Scientific) was added to each sample (55 °C for 3 h). In the next step, the trizol (Invitrogen) was used to dissociate nucleoprotein complexes (for at least 5 min). Chloroform (Merck) was added and the tubes were vortexed vigorously for 15 s. The samples were centrifuged at no more than 12,000*g* for 15 min at 4 °C and the aqueous phase was transferred to a fresh tube. The total RNA that was precipitated by mixing with isopropyl alcohol (Merck) was put at − 20 °C for at least 1 h. Then, it was centrifuged at 12,000*g* for 10 min at 4 °C. The RNA pellet was washed with 100% ethanol and dried at room temperature. Finally, the RNA pellet was dissolved in RNase-free water. The quality and quantity of extracted RNA were checked by agarose electrophoresis and Nanodrop. One microgram of the extracted RNA was used for cDNA synthesis using random hexamer and M-Mulv Reverse Transcriptase by *CinnaGen* First Strand *cDNA* synthesis Kit (*RT5201*), according to the kit instruction**.**

Real-time PCR

In situ gene expression of TNF-α (M1 hallmark) and TGF-β (M2 hallmark) in FFPE was measured using prepared cDNA by qPCR Master with low ROX Kit (Jena bioscience). Primers used for PCR were as follows: TNF-α, AGGAGGGAGAACAG CAACTC (forward) and TCATGCTTTCCGTGCTCATG (reverse); TGF-β CCTGCAAGACCATCGACATG (forward) and TGTTGTACAAAGCGAGCACC (reverse); for GAPDH as internal control, CAAGTTCAACGGCACAGTCA (forward) and CCCCATTTGATGTTAGCGGG (reverse). Cycling parameters were 95 °C for 2 min to activate DNA polymerase, followed by 35 cycles of denaturation 95 °C for 15 s, annealing and elongation 58 °C for 45 s (TGF-β) and 60 °C for 60 s (TNF-α). Specificity was confirmed by gel electrophoresis of products after real-time PCR and melting curve analysis.

Statistical analysis

Non-parametric Kruskal-Wallis test was used for analyzing data on wound healing percentage and H&E staining. The number of $iNOS^+$ and $CD163^+$ cells was assessed using one-way ANOVA and subsequently LSD post hoc test was

used to compare the means. TNF-α and TGF-β protein levels were analyzed by one-way ANOVA and then the Tukey test was used to compare the averages. Data on gene expression were analyzed by Rest-RG 2009 software.

Results

Ch nanohydrogel-AV characterization

The SEM images showed shape uniformity of synthesized AV-Ch as filamentous in (1:1 *v/w*), cubic (2:1 *v/w*), and spherical (3:1 *v/w*) and sizes smaller than 100 nm (Fig. 1).

The FTIR spectrum was recorded to study the interaction of Ch-sebacic acid and AV indicates encapsulation of AV into Ch nanohydrogel (Fig. 2). Peaks at 1568 cm^{-1} wavenumber and 1641 cm^{-1} of Fig. 2b indicate the amid binding between carboxyl of sebacic acid and amine of Ch. No peak was observed at 1715 cm^{-1} which indicates all carboxyl groups were bound to amine groups of sebacic acid. Additionally, the peak shift of 1622 cm^{-1} (N-H bending vibration) in AV spectra (Fig. 2a) to 1633 cm^{-1} in AV-Ch (Fig. 2c) suggests the physical hindrance of Ch for AV and the incorporation of AV into Ch nanohydrogel.

Antibacterial and antifungal assay

To further investigate the antimicrobial effects of Ch and AV, antimicrobial assay was tested using MIC, MBC, and MFC. As shown in Table 1a, AV-Ch (1:1 *v/w*) showed the greatest antibacterial effect against *Staphylococcus aureus* and *Salmonella typhi* (MIC = 250). The growth of *Salmonella typhi* was inhibited at MIC 500 of AV-Ch (2:1 *v/w*), Ch nanohydrogel, and AV. AV-Ch (3:1 *v/w*) represented the least antibacterial effects against the tested bacteria.

On the other hand, antifungal assay of AV/Ch (Table 1b) showed that AV-Ch (1:1 *v/w*) had the highest fungicidal and fungastatic (MFC, MIC = 250) activity on *Kluyveromyces marxianus* with MIC = 500 for AV and Ch against this fungus. *Candida albicans* growth was also inhibited with AV-Ch (1:1 *v/w*) at MIC = 500.

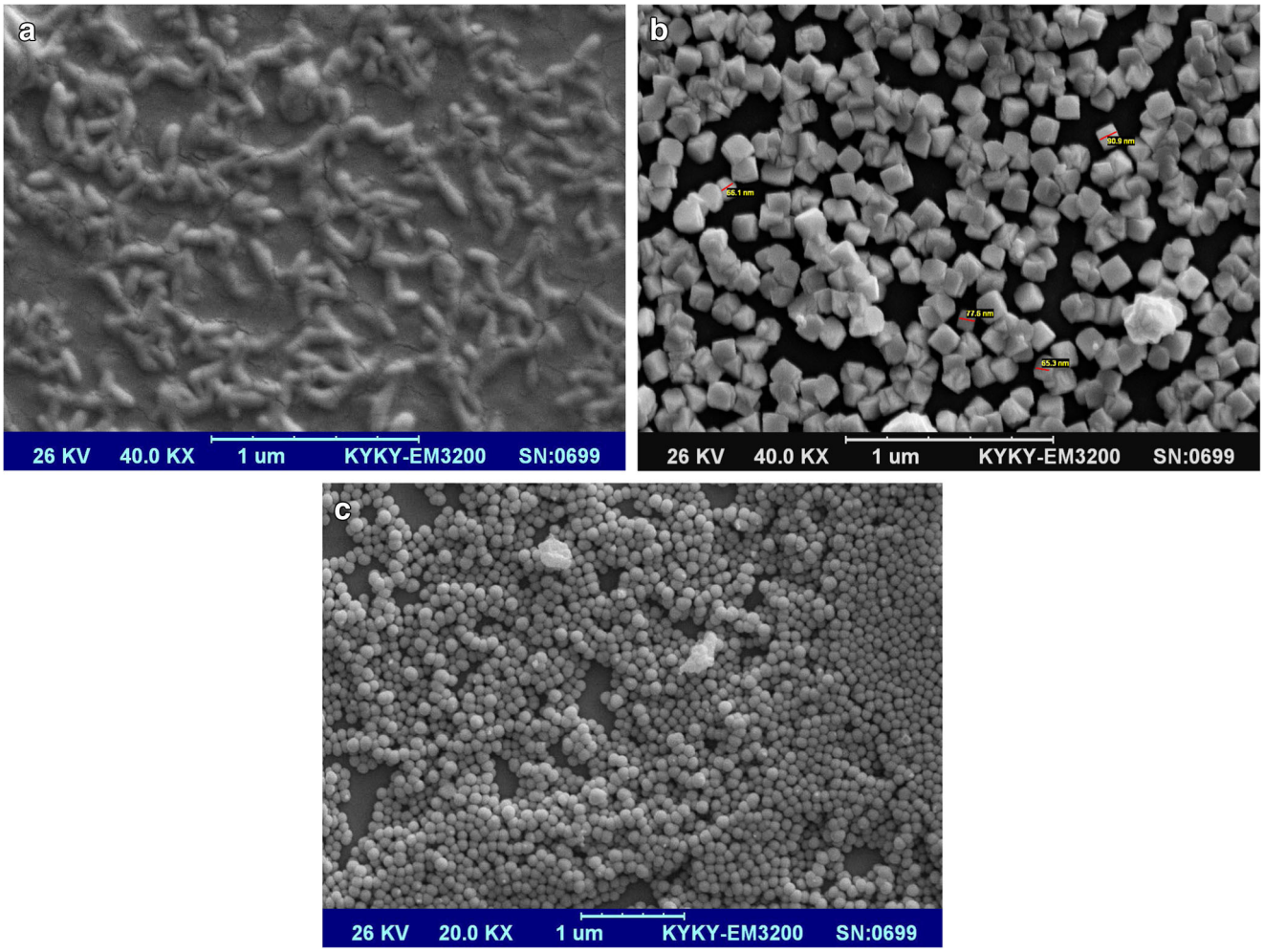

Fig. 1 SEM images of AV-Ch composites. To study the physical structure of AV-Ch, three different ratios of AV-Ch: **a** AV-Ch (1:1 *v/w*), **b** AV-Ch (2:1 *v/w*), and **c** AV-Ch (3:1 *v/w*) were produced and imaged by SEM. SEM, scanning electron microscope; AV, aloe vera; Ch, chitosan

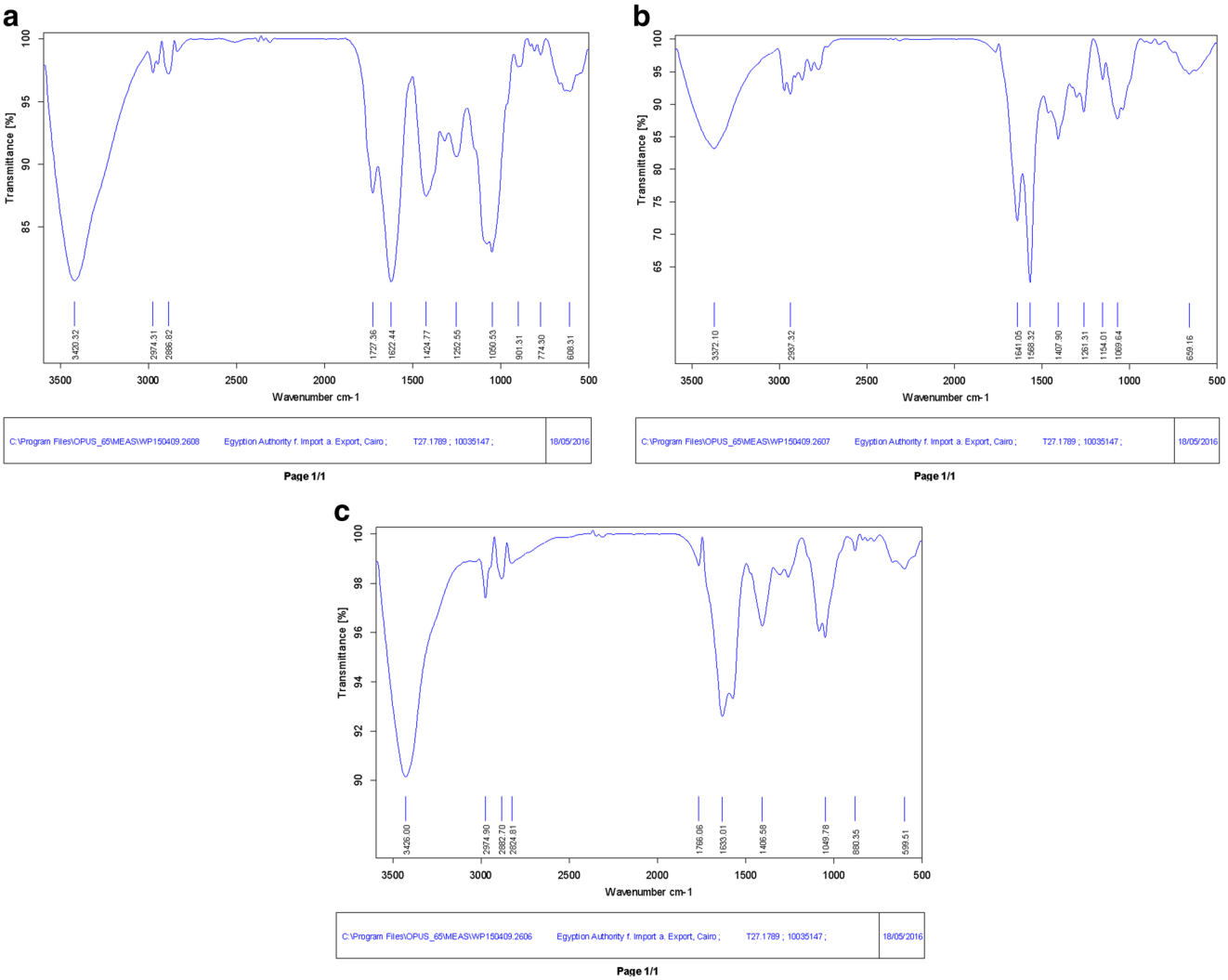

Fig. 2 FTIR of AV-Ch composites. Crosslinking of Ch and Av were analyzed by FTIR. **a** AV. **b** Ch-sebacic acid. **c** AV and Ch-sebacic acid (1:1 *v*/*w*). FTIR, Fourier transmission spectrometry; AV, aloe vera; Ch, chitosan

Percentage of wound healing

After wound creation in rats, each group was treated daily on the 3rd, 7th, 14th, 21st, and 28th days by AV, Ch, and different ratios of these compounds (Supplementary Fig. 1). Wound measurement was performed by point counting method [25, 26]. In order to measure the wound surface, we used point counting method using point grid (2 mm apart), and by using the following formula: Area = $\sum P \times a/p; \sum P$ where the total points fall on the wounded area, and a/p was the area per point. The percentage of wound healing was calculated by following formula;

$$\text{Percent of wound contraction} = (\text{initial wound area} - \text{current wound area})/\text{initial wound area} \times 100\%$$

Although all groups had a high rate of recovery and healing in comparison to the control group on the third and seventh days, only the AV-Ch (3:1 *v*/*w*) increased wound healing significantly compared to the control group ($P < 0.001$ and $P < 0.002$, respectively) (Fig. 3a). Moreover, the macroscopical analysis on the 14th and 21st days showed that although all treated groups were healed, wounds still persisted in the control (Fig. 3b). This is in accordance with significant enhanced healing of treated groups compare to control group ($P < 0.008$, $P < 0.01$) (Fig. 3a). As shown in Fig. 3a on the 28th day, all groups were recovered.

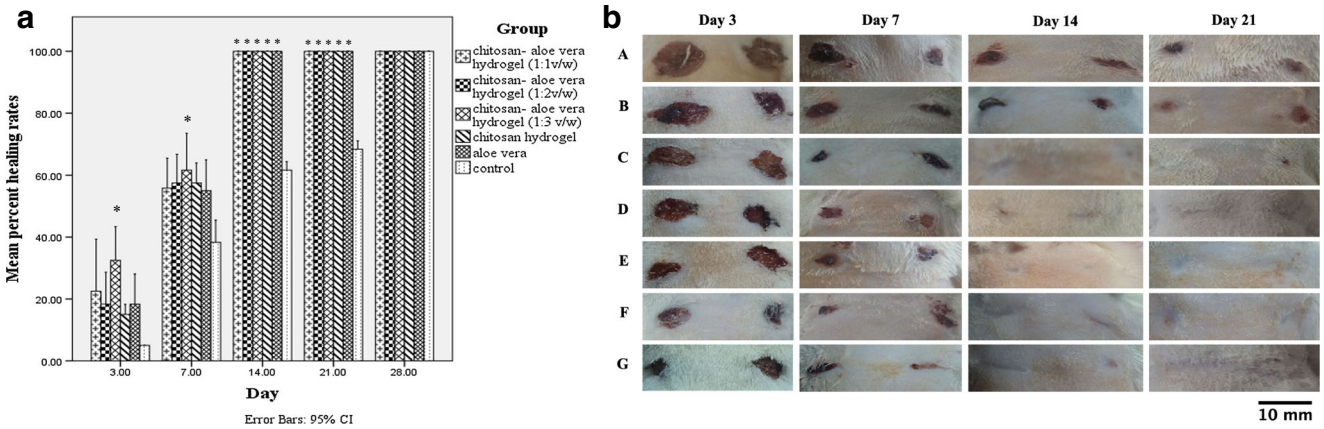

Fig. 3 Wound healing. **a** Percentage of wound healing; the percentage of wound healing was assessed on the 3rd, 7th, 14th, 21st, and 28th days after wound creation in rats. Mice were treated with aloe vera (AV), chitosan (Ch), AV-Ch (1:1 *v*/*w*), AV-Ch (2:1 *v*/*w*), AV-Ch (3:1 *v*/w), and normal saline (control). The star (*) shows a significant difference ($P < 0.05$) compared to the control group. Results are reported as mean ± standard error of the mean [4]. **b** Macroscopic image size of the wound in different groups. The rate of wound healing in (A) control groups, (B) AV, (C) Ch, (D) AV-Ch (1:1 *v*/*w*), (E) AV-Ch (2:1 *v*/w), and (F) AV-Ch (3:1 *v*/*w*). AV, aloe vera; Ch, chitosan

Histopathological studies

Microscopical evaluation of H&E stained wounds

After the preparation of tissue sections and H&E staining, each slide was examined for the quality of wound healing. For histopathology analysis, scoring scale from 0 to 4 (semi-quantitative method) was utilized (Table 2).

Accordingly, a representative picture of the scoring scale in H&E histological examination of the sections is shown in Fig. 4a. Namely, the presences of clots and exudate in the wound represent the initial phase and scored 0 (Fig. 4a(A)). Uncovered wound—with granular texture was given the score 1 (Fig. 4a(B)) and mainly occurred within 3 days (Fig. 4b). The inititiated coverage of the wound with granular texture, which was scored 2 (Fig. 4a(C)), was observed within 7 days of treated mice (Fig. 4b). However, the control groups, which lacks the wound cover, are still scored as 1. The complete coverage and the absence of skin lesion scored 3 (Fig. 4 a(D)) which is a representative of all treated groups on 14 days (in accordance with Fig. 3b) with the addition of control group on the 21st day (Fig. 4b). The normal derm and collagen (Fig. 4a(D)) scored 4 and is represented in AV-Ch (1:1 *v*/*w*) (group 1), AV-Ch (3:1 *v*/*w*) (group 3), and AV (group 5) (Fig. 4b). However, this increase in the quality of wound healing in treated groups compared to control was not statistically significant (Fig. 4b).

Table 2 Scoring scale for semi-quantitative analysis of H&E stained slides

Score	Quality
0	Clots (fibrin)-uncovered-exudate or acute inflammation
1	Uncovered wound—with granular texture
2	Covered wound—with granular tissue
3	Complete cover, fibrosis derma, no skin lesions
4	Normal-full coverage, dermal with normal collagen

Slides were scored according to wound covering/granular tissue, collagen deposition, and fibrosis criteria

Effect of AV-Ch nanohydrogel on M1 and M2 macrophages

Immunohistologic staining of the wound sections on the 3rd, 7th, and 14th days was done and the number of cells that expressed CD163 and iNOS was counted by optical microscopy. At least 100 random fields for each slide were counted and the average of positive cells was calculated and considered for statistical comparison.

AV-Ch nanohydrogel on M1 macrophage In order to determine the frequency of M1 macrophage, iNOS immunohistochemistry staining of wound was performed (Fig. 5). Microscopic evaluation (Fig. 5a) showed the gradual decrease of iNOS-positive cells over the time, from day 3 till day 14 in control, Ch, and AV-Ch (3:1 *v*/*w*)-treated groups. Additionally, increased $iNOS^+$ cells in AV-Ch (2:1 *v*/*w*) and AV were represented in the slides. Accordingly, statistical analysis of the average count of iNOS-positive cells on the third day showed that all treated groups except AV-Ch (2:1 *v*/*w*) had a significant reduction in iNOS-expressing cells ($P < 0.0001$). The results of the seventh day showed that $iNOS^+$ cells were increased in AV, AV-Ch (1:1 *v*/*w*), and AV-Ch (2:1 *v*/*w*) groups compared to the control group ($P < 0.0001$) (Fig. 5b).

AV-Ch nanohydrogel on M2 macrophage To elucidate the frequency of M2 macrophages, immunohistochemistry staining of CD163 was done on wound samples

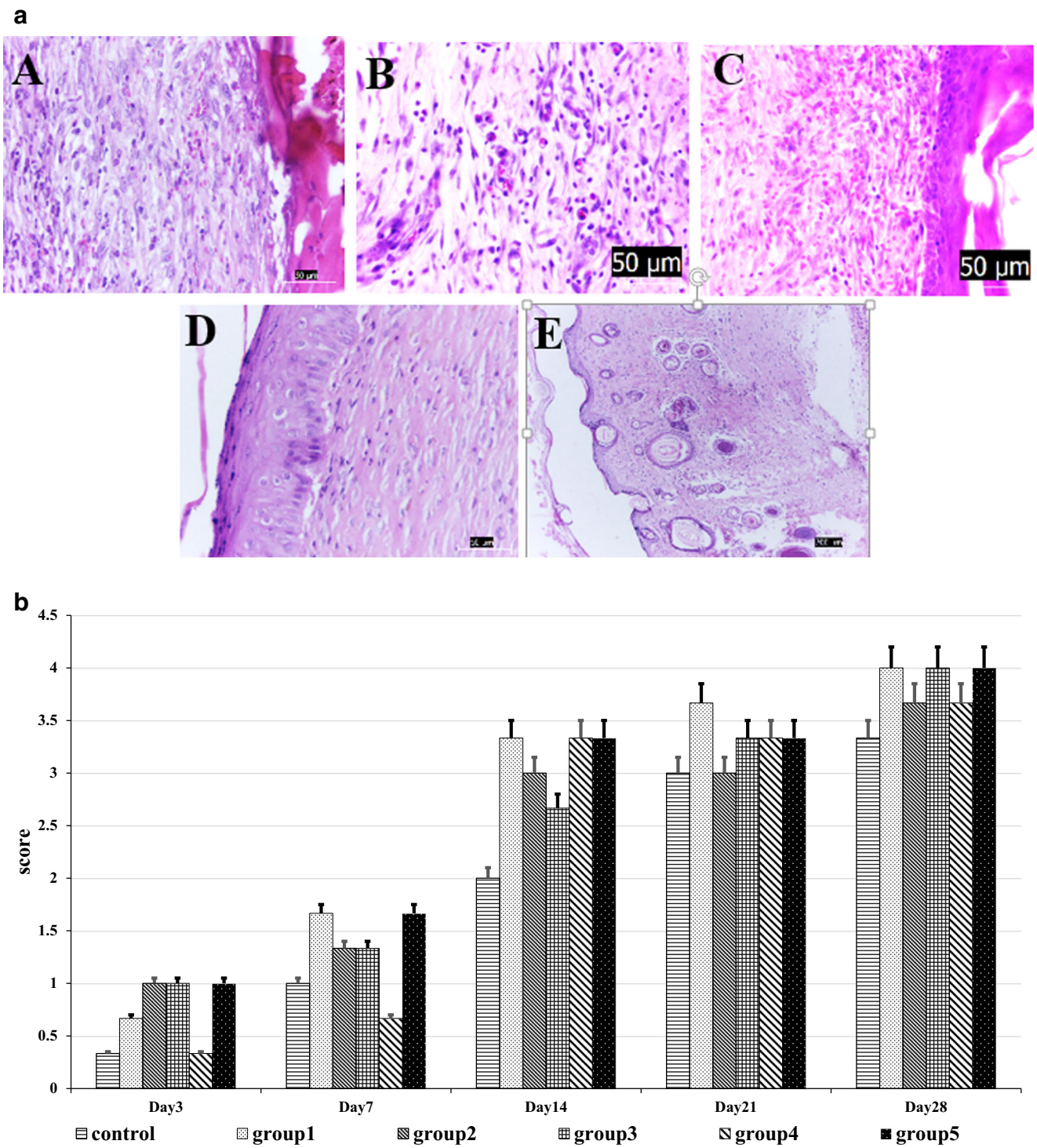

Fig. 4 H&E histological staining. **a** Microscopic images of the scores; H&E histological examination of the sections were performed by criteria and scaling that were defined in Table 2. Score 0, clots (fibrin)-uncovered-exudate or acute inflammation (A); score 1, uncovered wound—with granular texture (B); score 2, covered wound—with granular tissue (C); score 3, complete cover, fibrosis derm, no skin lesions (D); score 4, normal-full coverage, dermal with normal collagen (E). **b** Histopathological analysis based on the scales: effect of AV-Ch (1:1 *v*/*w*) (group 1), AV-Ch (2:1 *v*/*w*) (group 2), AV-Ch (3:1 *v*/*w*) (group 3), Ch (group 4), and AV (group 5) on score-based quality of wound healing. Results are reported as mean ± standard error of the mean. AV, aloe vera; Ch, chitosan

(Fig. 6). As shown in Fig. 6a, in contrast to AV and/or Ch-treated groups, the numbers of $CD163^+$ cells were very few in control groups and did not change over the inspected time (day 3–day 14). To further characterize the inter and intra differences of different groups, the statistical analysis of the average count of $CD163^+$ cells

on the 3rd and 14th days showed that the number of cells in all treated groups (except AV) was significantly higher compared to control group ($P < 0.0001$). However, on the seventh day, this increase was observed in all treatment groups including AV ($P < 0.0001$) (Fig. 6b).

Gene expression analysis for M1 and M2 cells in situ

To analyze in situ gene expression of TGF-β and TNF-α genes (selected M2 and M1 markers), real-time PCR in FFPE blocks was carried out.

TGF-β gene expression

Statistical analysis of TGF-β gene expression on the third day showed a significant decrease in AV group ($P < 0.03$) and on the 21st and 28th days, a significant reduction in Ch-treated groups compared to control group ($P < 0.00$) (Fig. 7).

TNF-α gene expression

The relative gene expression of TNF-α showed (Fig. 7) a significant reduction on the third day in AV and AV-Ch (1:1 *v*/*w*) (Fig. 7a, c) ($P < 0.00$) and on seventh day in AV and Ch groups (Fig. 7a, b) compared to the control group ($P < 0.001$). The results on the 14th and 28th showed that TNF-α gene expression in AV, Ch, and AV-Ch (3:1 *v*/*w*) groups decreased significantly (Fig. 7a, b, e) ($P < 0.00$, $P < 0.01$, and $P < 0.00$). Significant increase of the gene was observed at the third week in AV-Ch (1:1 *v*/*w*) and AV-Ch (2:1 *v*/*w*) (Fig. 7b, c) ($P < 0.00$).

Anti-inflammatory cytokines in serum

To investigate the changes in serum level of two major cytokines of M1 and M2, namely, TNF-α and TGF-β after euthanasia in each time point, the cytokine concentration was measured in serum of all groups by ELISA.

TGF-β concentration

As shown in Fig. 8a, the concentration of TGF-β was quite stable over the early phase of wound healing (3, 7, and 14 days treated groups). Although increased production in control and decreased in AV-Ch (3:1 *v*/*w*)-treated group was observed, however, these changes were not statistically significant. A significant difference of AV, AV-Ch (1:1 *v*/*w*), AV-Ch (2:1 *v*/*w*), AV-Ch (3:1 *v*/*w*) ($P < 0.004$, $P < 0.006$, $P < 0.006$, and $P < 0.004$), and control groups was observed mainly due to the decrease of TGF-β in control group. On the 28th day, the enhanced concentration of TGF-β in control group resulted in significant differences with AV, Ch, AV-Ch (1:1 *v*/*w*), AV-Ch (2:1 *v*/*w*), and AV-Ch (3:1 *v*/*w*)-treated groups ($P < 0.01$, $P < 0.001$, $P < 0.01$, $P < 0.01$, and $P < 0.01$) (Fig. 8a).

TNF-α concentration

The results of TNF-α concentration showed a general increase on the third day, inflammatory phase, in most groups and it declined with some variability over the days 7, 14, and 21. However, these changes were not statistically significant. On the 28th day in AV, Ch, AV-Ch (1:1 *v*/*w*), AV-Ch (2:1 *v*/*w*), and control groups decreased significantly compared to AV-Ch (3:1 *v*/*w*) group ($P < 0.002$, $P < 0.001$, $P < 0.001$, $P < 0.03$, and $P < 0.002$) (Fig. 8b).

Discussion

Indeed, effective and timely transition of M1 to M2 in wound healing is associated with tissue regeneration whereas an extended M1 response or excessive transition to M2 delays wound healing [5]. Importantly, exploiting natural polymers such as Ch and AV could modulate this process and promote tissue regeneration of wound. According to previous studies, the combination of Ch with AV increased the number of multinuclei and mononuclear cells, proliferation of fibroblasts, angiogenesis, collagen production, epithelialization, and antimicrobial activity [27, 28]. However, detailed cellular and molecular mechanisms, especially in macrophages, are unclear. Additionally, nanohydrogel composition of Ch would result in more efficient treatment since most biological processes occur at the nanometer scale [29]. Therefore, in this study, separate and/or combined effects of Ch nanohydrogel and AV were investigated on the phenotype and functions of M1 and M2.

Accordingly, first the physical and chemical structure of the prepared AV/Ch nanohydrogel was evaluated using SEM and FTIR, respectively. The particles showing size less than 100 nm with the uniformity of AV and Ch at different ratios confirming the nanostructure of the products. Although at different ratios of AV to Ch different physical structures were observed, for instance AV (3:1 *v*/*w*) spherical versus cubic at AV (2:1 *v*/*w*), however, the uniformity and homogeneity did not change and the shape was affected by different concentrations of AV.

Furthermore, the chemical structure analysis by FTIR proved the chemical modification of Ch by sebacic acid through amine-carboxyl interactions to form nanohydrogel. Shift in 1622 cm^{-1} wave of AV to 1633 cm^{-1} wave in AV-nanohydrogel Ch implies that interaction of Ch and AV has occurred.

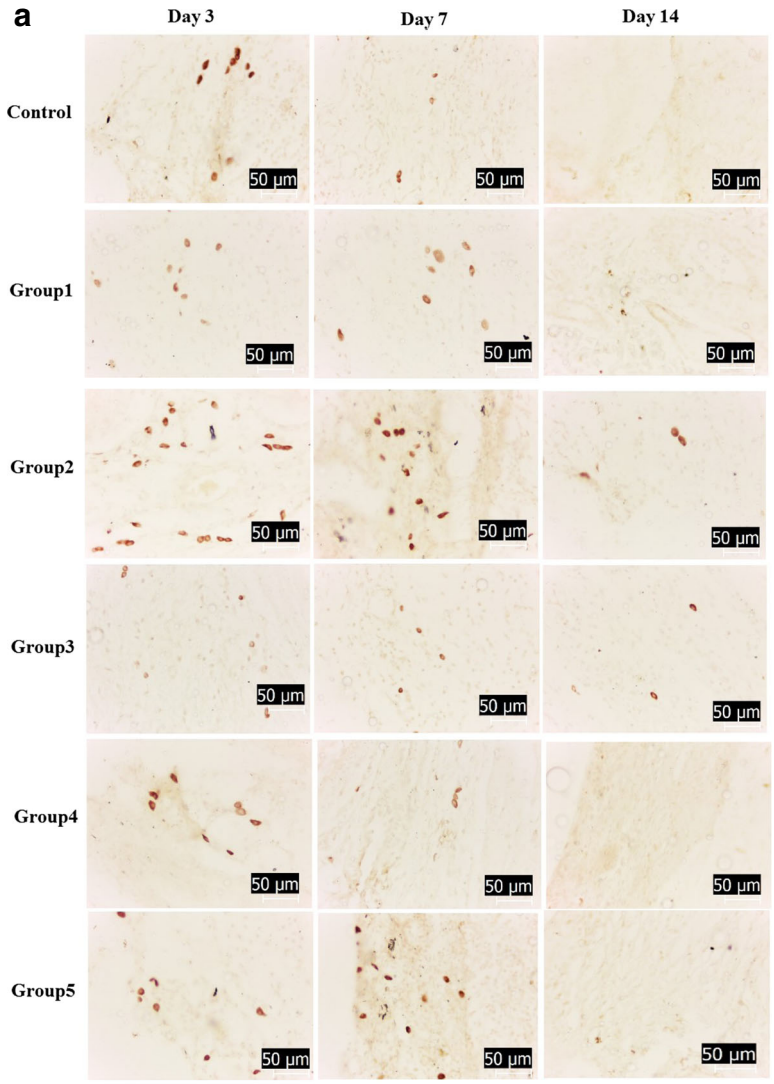
a
Day 3
Day 7
Day 14
Control
Group1
Group2
Group3
Group4
Group5
50 μm

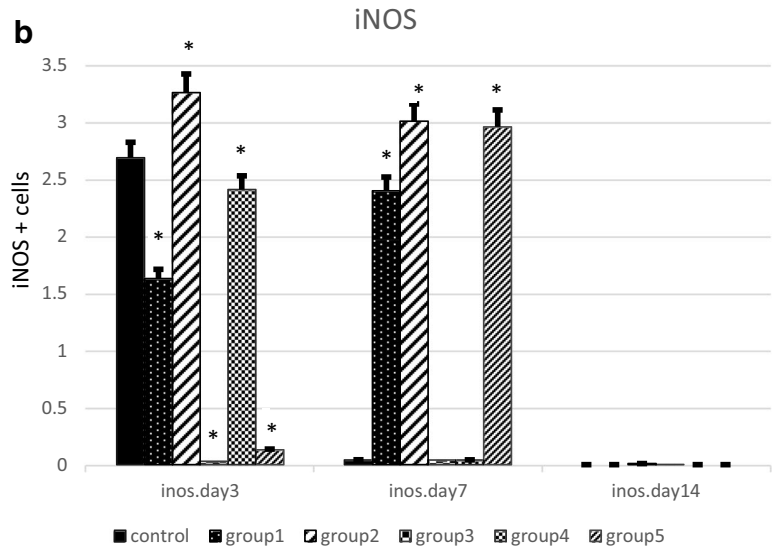
b
iNOS
iNOS + cells
3.5
3
2.5
2
1.5
1
0.5
0
inos.day3
inos.day7
inos.day14
control
group1
group2
group3
group4
group5

◀ **Fig. 5** Immunohistochemistry of iNOS in FFPE sections. FFPE sections of each treated group at different intervals (3rd, 7th, 14th days) were prepared and stained by iNOS Ab. **a** Microscopic image of iNOS$^+$ cells. AV-Ch (1:1 *v/w*) (group 1), AV-Ch (2:1 *v/w*) (group 2), AV-Ch (3:1 *v/w*), Ch (group 4), and AV (group 5). **b** The number of cells with the iNOS marker. Immunohistochemistry of wound tissues in AV-Ch (1:1 *v/w*), AV-Ch (2:1 *v/w*), AV-Ch (3:1 *v/w*) (group 3), Ch (group 4), and AV (group 5) and control on the 3rd, 7th, and 14th. Results are reported as mean ± standard error of the mean. The star (*) shows a significant difference ($P < 0.05$) compared to the control group AV, aloe vera; Ch, chitosan; FFPE, formalin-fixed paraffin-embedded

Following the structural analysis, we aimed to study the antimicrobial activity of the compounds. Importantly, the risk of microbial contamination of the wound delays the healing process [22]. Given this, and according to previous studies showing antimicrobial activity of AV [18] and Ch [30], the compounds were assessed for antimicrobial features. Findings indicated that the most effectiveness of AV-Ch (1:1 *v/w*) in terms of inhibitory growth of *Salmonella typhi* and *Staphylococcus aureus* bacteria (as two main gram positive and negative skin bacteria which could result in wound infection) and fungicidal and fungistatic effects for *Kluyveromyces marxianus*. Importantly, *Salmonella typhi* was the most sensitive bacteria to all tested AV and Ch compounds (except for AV-Ch (3:1 *v/w*). *Candida albicans* growth was also inhibited with AV-Ch (1:1 *v/w*) at MIC = 500. Overall, these findings suggest the optimum antimicrobial feature of AV and Ch exerts in equal ratio of these compounds, i.e., AV-Ch (1:1 *v/w*).

In the next step, the wound healing capacity was tested on rats treated with either AV and/or Ch in different ratios as well as different time points. The results of macroscopic examination showed the fastest healing occurred with the highest concentration of AV starting on the third day. This is in agreement with earlier studies showing that wound healing at 100% concentration of AV was significantly higher than 12.5% concentration [31]. Thus, the recovery rate is associated proportionally with the higher AV concentration. Interestingly, it has been shown that the use of Ch [22] or in combination with AV [28] increases wound healing, homeostasis, and epithelialization that is in agreement with better wound healing in combined groups in present study.

Semi-quantitative analysis of H&E stained sections showed that the improvement of wound healing on the third and seventh days in all treated groups (except Ch) and on the 14th and 28th days in all group compared to control group. However, none of these differences was statistically significant, which might be due to the semi-quantitative assessment of the sections. Additionally, the initial wound size (1 cm) was lower than study tested Ch on 4 cm initial wound size [32] . Following 14 days of AV treatment, fibroblast number increased. This resulted into enhanced collagen production and increased density of collagen fibers in AV-treated groups. The increased fibroblasts caused by AV in the current study are in agreement with previous report [33]. However, decreased collagen levels on days 21 and 28 indicate normalization of the dermis.

Histologically, the effect of Ch on the quality of wound healing begins from the first week due to increased number of fibroblasts and epithelization level. This phenomenon could be intensified from the second week, with developed granular layer and increased fibroblasts and epithelization on the 20th day [34], which justifies the effects observed in our study with Ch. The findings support that AV improves wound healing when combined with Ch.

Immunohistochemistry on the third day showed that AV-Ch (2:1 *v/w*)-treated cells are still in transition from M1 to M2. This could be due to improper or even suppressive ratio of AV/Ch which caused high presence of both high iNOS$^+$ and CD163$^+$ cells. However, other groups passed the M1 stage on the third day and entered the M2 phase with less iNOS$^+$ and more CD163$^+$ cells in all AV-Ch combinations and Ch. Noticeably, AV treatment showed reduction in CD163 and iNOS, indicating the primary suppressive effects of AV. Reduced inflammation came with the highest dose of AV in AV-Ch (3:1 *v/w*), which might be due to the dual effects of AV. It has been shown that treating human monocyte with Aloeride (AV's polysaccharide) for 2 h increases NFKβ and IL-1β and TNF-α mRNA [35], resulting in differentiation of monocytes into M1 macrophages.

Immunohistochemistry results on the 7th and 14th days in AV-Ch (3:1 *v/w*) and Ch-treated groups showed a balance toward M2 while other groups were still in transitional stage from M1 to M2. An interesting finding of M1/M2 on the 14th day was related to AV-Ch (1:1 *v/w*) group, which was shifting the balance toward M2 (such as its effect on day 3); this implies multiple transitions of M1 and M2 occur during healing and require further investigation. Anti-inflammatory effects of Ch were reported in Ch-treated macrophages via increased production of TGF-β and IL-10 and decreased MHCII, CD86, and as TNF-α [6]. It could be concluded that AV itself could not shift the balance between M1 and M2, which further shows the beneficial effect of combing with Ch.

It has been found that the AV and Ch increases TGF-β gene expression and consequently increases wound healing [36, 37] by epithelialization, the formation of new veins, granular tissue, fibroblast proliferation, and the production of ECM components [38]. TGF-β has anti-inflammatory roles in the early/late stages of wound healing. Additionally, TNF-α has harmful and beneficial effect on wound healing which is time and dosage dependent. Increased TNF-α reduces collagen formation and tissue regeneration while reduced TNF-α and TNFR-α induces M2 macrophages [39, 40].

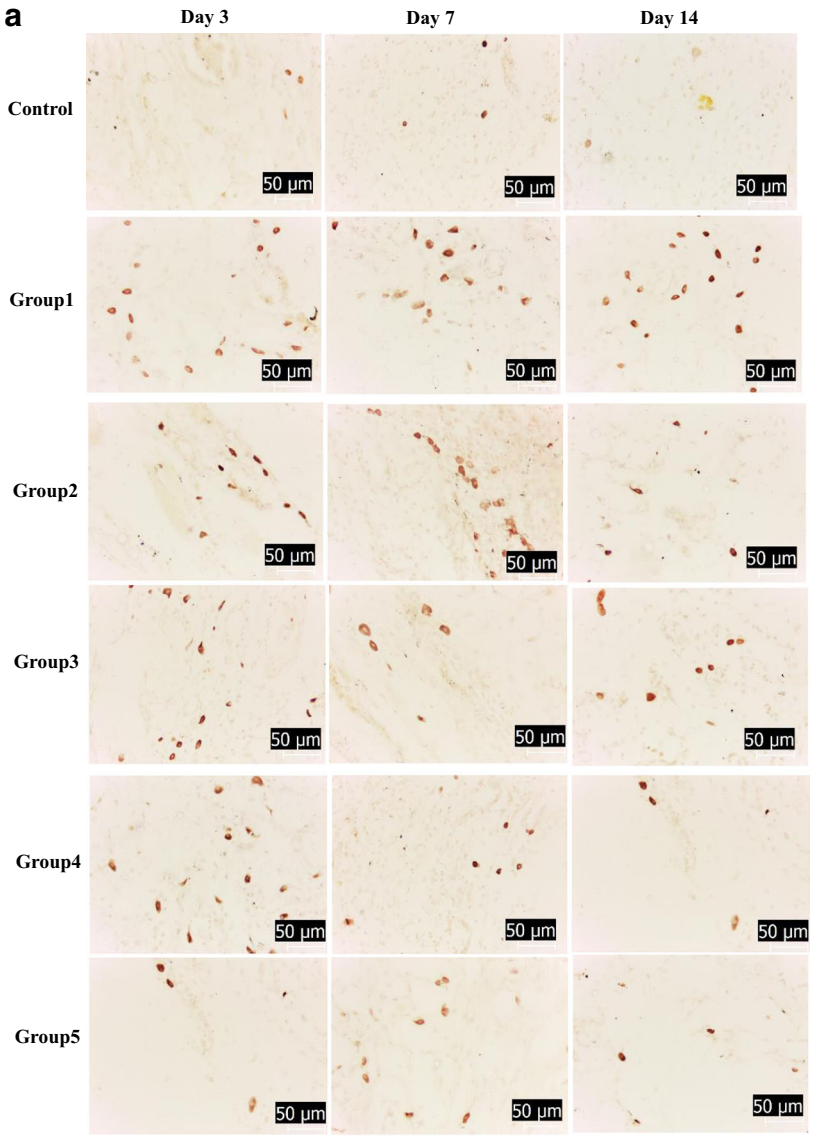
a
Day 3
Day 7
Day 14
Control
Group1
Group2
Group3
Group4
Group5
50 μm

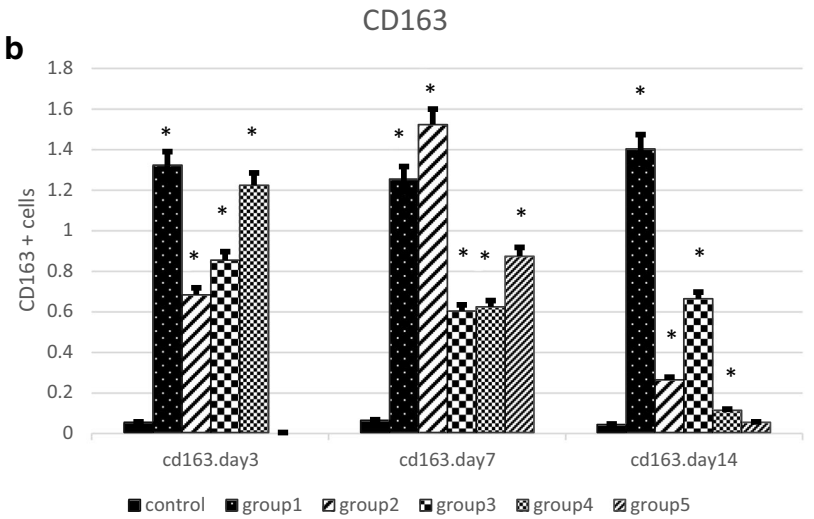
b
CD163
CD163 + cells
1.8
1.6
1.4
1.2
1
0.8
0.6
0.4
0.2
0
cd163.day3
cd163.day7
cd163.day14
control
group1
group2
group3
group4
group5

◀ **Fig. 6** Immunohistochemistry of CD163 in FFPE sections. FFPE sections of each treated group at different intervals (3rd, 7th, 14th days) were prepared and stained by CD163 Ab. **a** Microscopic image of $CD163^{+}$ cells. AV-Ch (1:1 *v/w*) (group 1), AV-Ch (2:1 *v/w*) (group 2), AV-Ch (3:1 *v/w*), Ch (group 4), and AV (group 5). **b** The number of CD163 marker cells. Immunohistochemistry of FFPE sections in AV-Ch (1:1 *v/w*) (group 1), AV-Ch (2:1 *v/w*) (group 2), AV-Ch (3:1 *v/w*), Ch (group 4), and AV (group 5) and control on the 3rd, 7th, and 14th days. Results are reported as mean ± standard error of the mean. The star (*) shows a significant difference ($P < 0.05$) compared to the control group. AV, aloe vera; Ch, chitosan; FFPE, formalin-fixed paraffin-embedded

Gene expression analysis of TNF-α on the third day was in agreement of immunohistochemical results that showed Ch and AV-Ch (1:1 *v/w*) reduced the expression of TNF-α gene and iNOS. Furthermore, the application of AV simultaneously decreased TGF-β and TNF-α genes and both iNOS and CD163 on the third day. It has been shown that AV has a dosage-dependent anti-inflammatory effect on human macrophages in vitro by reducing inflammatory cytokines such as TNF-α, IL-1, and IL-6. The reduction was greater in AV 3% versus

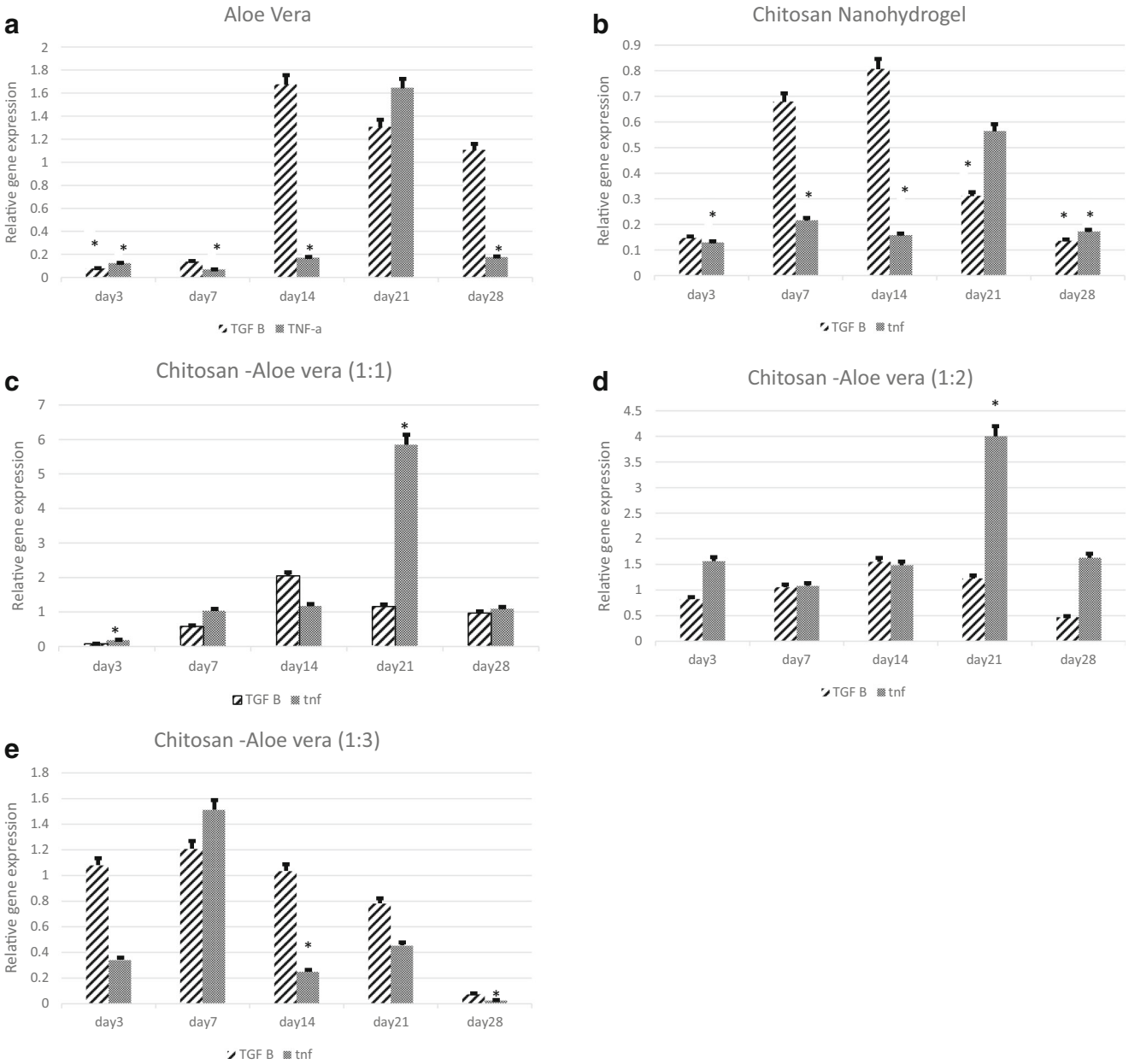

Fig. 7 TGF-β and TNF-α gene expression. Real-time PCR was performed in FFPE blocks of all treated groups in different intervals (3rd, 7th, 14th, 21st, 28th days) to determine the expression of TGF-β and TNF-α ratio. GAPDH was chosen for housekeeping gene with the expression level of one (GAPDH bars are not shown). The star (*) shows a significant difference. ($P < 0.05$) compared to the control group. Results are reported as mean ± standard error of the mean. **a** AV. **b** Ch nanohydrogel. **c** AV and Ch (1:1 *v/w*). **d** AV and Ch nanohydrogel (2:1 *v/w*). **e** AV and Ch nanohydrogel (3:1 *v/w*). AV, aloe vera; Ch, chitosan

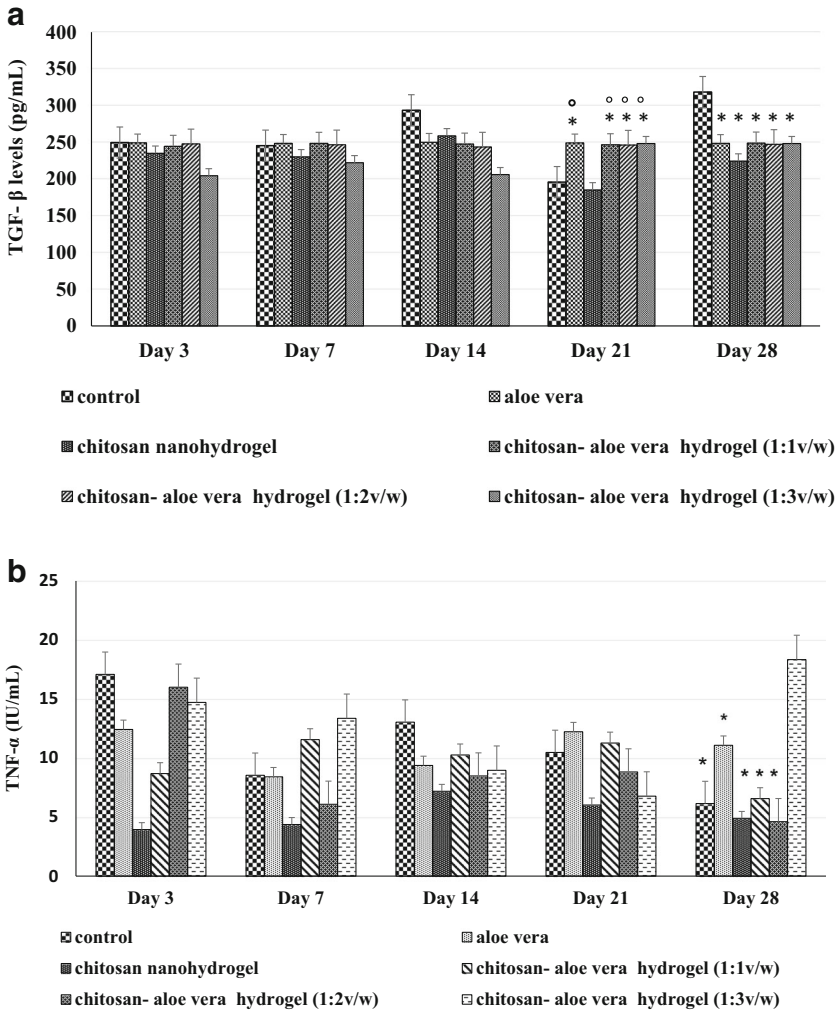

Fig. 8 TGF-β and TNF-α protein concentration in serums of wounded mice. After killing of mice in different intervals (3rd, 7th, 14th, 21st, 28th days), serum was collected and cytokines concentrations were measured by ELISA. **a** Effect of AV/Ch on TGF-β protein concentrations. The star (*) shows a significant difference ($P < 0.05$) compared to the control and the character (o) shows significant difference compared to Ch. **b** Effect of AV/Ch on TNF-α protein concentrations. Results are reported as mean ± standard error of the mean. The star sign (*) shows a significant difference ($P < 0.05$) compared to the AV-Ch (3:1 *v*/*w*). AV, aloe vera; Ch, chitosan

1% concentration. However, in THP-1 cells, the reduction of inflammatory cytokines was observed at higher dosages of AV (10%) [19]. Therefore, the difference in cell types affects the outcome, which needs to be considered when comparing the results.

Studying the delayed phase of wound healing in the third and fourth weeks showed a decreased in TGF-β gene expression in the Ch group and decreased TGF-β protein in the fourth week in all groups compared to control. This reduction is beneficial at this stage because it helps prevent scar formation and leads to normal tissue repair. Another study showed increased TGF-β gene in the initial phase and delayed phase (seventh day) by Ch treatment on BALB/C mouse wound healing [37]. As they did not analyze TGF-β gene on the 28th day, a corresponding comparison could not be made. However, nanohydrogel composition of Ch in our study causes gradual releases of material and prolongs its effect.

Comparison of TNF-α and TGF-β gene and protein data might be misleading because of in situ assessment of genes and systemic measurement of proteins in serum. Cytokine measurements in serum require a higher concentration of molecules and are not directly related to secretion of macrophages within the wound, while the real-time PCR shows sensitive measurement at specific time in situ. Furthermore, the interval between the conversions of the gene to the protein should also be considered in interpretation of the results. Future experiments are required to assess TNF-α and TGF-β proteins in situ.

In conclusion

Generally, the observed effects of AV on tissue regeneration were mainly anti-inflammatory. However, AV-Ch combination modulates M1–M2 responses leading to improved wound healing. The optimum recovery was observed following AV-Ch (1 and 3:1 *v*/*w*) and Ch treatment by decreasing M1 after 3 days and increasing M2 after 14.

This is the first study that analyzes Ch's nanohydrogel form, and/or AV's impact on M1 and M2 in vivo in regard to wound healing. Further studies are required to investigate

comprehensive phenotyping of classical and alternative macrophages plus their function.

Acknowledgments This work was financially supported by Lorestan University of Medical Sciences, Iran (Grant No. A-10-1471-3). We are thankful to Dr. Mandana Beigi Boroujeni for her helpful advice on histological analysis. We would like to give our appreciation to Dr. Saeed Veiskarami for statistical analysis and Behnam Ashrafi for antimicrobial analysis.

Compliance with ethical standards

Conflict of interest The authors declare that they have no conflict of interest.

References

1. Mantovani A, Sozzani S, Locati M, Allavena P, Sica A. Macrophage polarization: tumor-associated macrophages as a paradigm for polarized M2 mononuclear phagocytes. Trends Immunol. 2002;23(11):549–55.
2. Mahdavian Delavary B, van der Veer WM, van Egmond M, Niessen FB, Beelen RH. Macrophages in skin injury and repair. Immunobiology. 2011;216(7):753–62. https://doi.org/10.1016/j.imbio.2011.01.001.
3. Sridharan R, Cameron AR, Kelly DJ, Kearney CJ, O'Brien FJ. Biomaterial based modulation of macrophage polarization: a review and suggested design principles. Mater Today. 2015;18(6):313–25. https://doi.org/10.1016/j.mattod.2015.01.019.
4. Boersema GS, Grotenhuis N, Bayon Y, Lange JF, Bastiaansen-Jenniskens YM. The effect of biomaterials used for tissue regeneration purposes on polarization of macrophages. BioResearch Open Access. 2016;5(1):6–14. https://doi.org/10.1089/biores.2015.0041.
5. Brown BN, Badylak SF. Expanded applications, shifting paradigms and an improved understanding of host–biomaterial interactions. Acta Biomater. 2013;9(2):4948–55.
6. Oliveira MI, Santos SG, Oliveira MJ, Torres AL, Barbosa MA. Chitosan drives anti-inflammatory macrophage polarisation and pro-inflammatory dendritic cell stimulation. Eur Cells Mater. 2012;24:136–52; discussion 152-133.
7. Almeida CR, Serra T, Oliveira MI, Planell JA, Barbosa MA, Navarro M. Impact of 3-D printed PLA- and chitosan-based scaffolds on human monocyte/macrophage responses: unraveling the effect of 3-D structures on inflammation. Acta Biomater. 2014;10(2):613–22. https://doi.org/10.1016/j.actbio.2013.10.035.
8. Ribeiro MP, Espiga A, Silva D, Baptista P, Henriques J, Ferreira C, et al. Development of a new chitosan hydrogel for wound dressing. Wound Repair Regen. 2009;17(6):817–24. https://doi.org/10.1111/j.1524-475X.2009.00538.x.
9. Alves NM, Mano JF. Chitosan derivatives obtained by chemical modifications for biomedical and environmental applications. Int J Biol Macromol. 2008;43(5):401–14. https://doi.org/10.1016/j.ijbiomac.2008.09.007.
10. Fong D, Hoemann CD. Chitosan immunomodulatory properties: perspectives on the impact of structural properties and dosage. Future science OA. 2018;4(1):Fso225. https://doi.org/10.4155/fsoa-2017-0064.
11. Peluso G, Petillo O, Ranieri M, Santin M, Ambrosio L, Calabro D, et al. Chitosan-mediated stimulation of macrophage function. Biomaterials. 1994;15(15):1215–20.
12. Dalwadi C, Patel G. Application of nanohydrogels in drug delivery systems: recent patents review. Recent Patents Nanotechnol. 2015;9(1):17–25.
13. Hamman JH. Composition and applications of aloe vera leaf gel. Molecules (Basel, Switzerland). 2008;13(8):1599–616.
14. Schmidt JM, Greenspoon JS. Aloe vera dermal wound gel is associated with a delay in wound healing. Obstet Gynecol. 1991;78(1):115–7.
15. Silva SS, Caridade SG, Mano JF, Reis RL. Effect of crosslinking in chitosan/aloe vera-based membranes for biomedical applications. Carbohydr Polym. 2013;98(1):581–8. https://doi.org/10.1016/j.carbpol.2013.06.022.
16. Reynolds T, Dweck AC. Aloe vera leaf gel: a review update. J Ethnopharmacol. 1999;68(1–3):3–37.
17. Farahnejad Z, Ghazanfari T, Yaraee R. Immunomodulatory effects of aloe vera and its fractions on response of macrophages against Candida albicans. Immunopharmacol Immunotoxicol. 2011;33(4):676–81. https://doi.org/10.3109/08923973.2011.560158.
18. Bernardes I, Felipe Rodrigues MP, Bacelli GK, Munin E, Alves LP, Costa MS. Aloe vera extract reduces both growth and germ tube formation by Candida albicans. Mycoses. 2012;55(3):257–61. https://doi.org/10.1111/j.1439-0507.2011.02079.x.
19. Budai MM, Varga A, Milesz S, Tozser J, Benko S. Aloe vera downregulates LPS-induced inflammatory cytokine production and expression of NLRP3 inflammasome in human macrophages. Mol Immunol. 2013;56(4):471–9. https://doi.org/10.1016/j.molimm.2013.05.005.
20. Inpanya P, Faikrua A, Ounaroon A, Sittichokechaiwut A, Viyoch J. Effects of the blended fibroin/aloe gel film on wound healing in streptozotocin-induced diabetic rats. Biomed Mater (Bristol, England). 2012;7(3):035008. https://doi.org/10.1088/1748-6041/7/3/035008.
21. Park KR, Nho YC. Preparation and characterization by radiation of poly(vinyl alcohol) and poly(N-vinylpyrrolidone) hydrogels containing aloe vera. J Appl Polym Sci. 2003;90(6):1477–85. https://doi.org/10.1002/app.12656.
22. Ahmed S, Ikram S. Chitosan based scaffolds and their applications in wound healing. Achiev Life Sci. 2016;10(1):27–37. https://doi.org/10.1016/j.als.2016.04.001.
23. REX JH, Alexander BD, Andes D, Arthington-skaggs B, Brown SD, Chaturveli V, et al. In: Wayne P, editor. Reference method for broth dilution antifungal susceptibility testing of filamentous fungi; approved standard. USA: Clinical and Laboratory Standards Institute; 2008.
24. Ma Z. Total RNA extraction from formalin-fixed, paraffin-embedded (FFPE) blocks. Bio-protocol. 2012;2(7):e161. https://doi.org/10.21769/BioProtoc.161.
25. Bahmer FA. Wound measurement made truly simple by point counting. Arch Dermatol. 1999;135(8):991-a-992. https://doi.org/10.1001/pubs.ArchDermatol.-ISSN-0003-987x-135-8-dlt0899.
26. Rafiee S, Nekouyian N, Hosseini S, Sarabandi F, Chavoshi-Nejad M, Mohsenikia M, et al. Effect of topical Linum usitatissimum on full thickness excisional skin wounds. Trauma Mon. 2017;22(6):e64930. https://doi.org/10.5812/traumamon.39045.
27. Ranjbar R, Yousefi A. Effects of aloe vera and chitosan nanoparticle thin-film membranes on wound healing in full thickness infected wounds with methicillin resistant Staphylococcus aureus. Bull Emerg Trauma. 2018;6(1 JAN):8–15.
28. Ammayappan L, Moses JJ. Study of antimicrobial activity of aloevera, chitosan, and curcumin on cotton, wool, and rabbit hair. Fibers Polym. 2009;10(2):161–6.
29. Wang EC, Wang AZ. Nanoparticles and their applications in cell and molecular biology. Integr Biol. 2014;6(1):9–26.
30. Raafat D, Sahl H-G. Chitosan and its antimicrobial potential—a critical literature survey. Microb Biotechnol. 2009;2(2):186–201. https://doi.org/10.1111/j.1751-7915.2008.00080.x.

31. Hajhashemi V, Ghannadi A, Heidari A. Anti-inflammatory and wound healing activities of Aloe littoralis in rats. Res Pharm Sci. 2012;7(2):73–8.
32. Archana D, Dutta J, Dutta P. Evaluation of chitosan nano dressing for wound healing: characterization, in vitro and in vivo studies. Int J Biol Macromol. 2013;57:193–203.
33. Chithra P, Sajithlal GB, Chandrakasan G. Influence of aloe vera on collagen characteristics in healing dermal wounds in rats. Mol Cell Biochem. 1998;181(1):71–6. https://doi.org/10.1023/a:1006813510959.
34. Azad AK, Sermsintham N, Chandrkrachang S, Stevens WF. Chitosan membrane as a wound-healing dressing: characterization and clinical application. J Biomed Mater Res B Appl Biomater. 2004;69(2):216–22.
35. Pugh N, Ross SA, ElSohly MA, Pasco DS. Characterization of Aloeride, a new high-molecular-weight polysaccharide from aloe vera with potent immunostimulatory activity. J Agric Food Chem. 2001;49(2):1030–4.
36. Takzaree N, Hadjiakhondi A, Hassanzadeh G, Rouini MR, Manayi A, Zolbin MM. Transforming growth factor-beta (TGF-beta) activation in cutaneous wounds after topical application of aloe vera gel. Can J Physiol Pharmacol. 2016;94(12):1285–90. https://doi.org/10.1139/cjpp-2015-0460.
37. Baxter RM, Dai T, Kimball J, Wang E, Hamblin MR, Wiesmann WP, et al. Chitosan dressing promotes healing in third degree burns in mice: gene expression analysis shows biphasic effects for rapid tissue regeneration and decreased fibrotic signaling. J Biomed Mater Res A. 2013;101(2):340–8.
38. Finnson KW, McLean S, Di Guglielmo GM, Philip A. Dynamics of transforming growth factor beta signaling in wound healing and scarring. Adv Wound care. 2013;2(5):195–214.
39. Rapala K. The effect of tumor necrosis factor-alpha on wound healing. An experimental study. In: Annales chirurgiae et gynaecologiae. Supplementum; 1996. p. 1–53.
40. Wu X, Xu W, Feng X, He Y, Liu X, Gao Y, et al. TNF-a mediated inflammatory macrophage polarization contributes to the pathogenesis of steroid-induced osteonecrosis in mice. Int J Immunopathol Pharmacol. 2015;28(3):351–61.